Revista de la Sociedad Geológica de España 29 (2)

ISSN (versión impresa): 0214-2708
ISSN (Internet): 2255-1379

MINERALOGICAL AND GEOCHEMICAL CHARACTERIZATION OF SÉRIE NEGRA BLACK QUARTZITES, COIMBRA-CORDOBA SHEAR ZONE, EAST PORTUGAL

Caracterización mineralógica y geoquímica de las cuarcitas negras de la Serie Negra, zona de cizalla Coimbra-Córdoba, Este de Portugal

Daniel P. S. de Oliveira[1], Teresa P. Silva[1]and Fernanda Guimarães[2]

[1] *Mineral Resources and Geophysics Research Unit, Laboratório Nacional de Energia e Geologia (LNEG), Estrada da Portela-Zambujal, Apartado 7586, 2610-999 Amadora, Portugal; daniel.oliveira@lneg.pt; teresa.pena@lneg.pt*

[2] *Mineral Science and Technology Unit, Laboratório Nacional de Energia e Geologia (LNEG), Rua da Amieira, Apartado 1089, 4466-901 S. Mamede de Infesta, Portugal; fernanda.guimaraes@lneg.pt*

Abstract*: The Coimbra-Cordoba Shear Zone (CCSZ) forms the boundary that separates two distinct tectonostratigraphic areas, the Ossa Morena (to the S) and Central Iberian Zones (to the N) across Iberia. Within this shear zone outcrop the gold-bearing Série Negra rocks made up of essentially metasedimentary units with schists, quartzites, arenites, greywackes, limestones including amphibolites and felsic volcanic rocks. The black quartzites, characteristic of this package, show recrystallization, often exhibiting undulose extinction and microstylolites, and embayed and irregular crystal faces registering the effects of the local tectonic history. Their dark color probably results from the inclusion of thin C-rich flakes in thin micrometric layers. Although previously classified as cherts, evidence points to their having a likely detrital source and geochemical protolith signatures of the source geological setting point to a quartzose sedimentary provenance. Their geochemistry also suggests that the samples studied originated in a passive margin setting although some samples tend to suggest oceanic to continental paleo-arc settings with Th/Sc and La/Th ratios pointing to a probable basic to intermediate protolith, which is corroborated mineralogically.*

Key-words: *Coimbra-Cordoba Shear Zone, Série Negra, black quartzites, C-rich flakes.*

Resumen*: En Iberia, la Zona de Cizalla de Coimbra-Córdoba (ZCCC) constituye el límite entre dos áreas tectonoestratigráficas distintas, las Zonas de Ossa Morena (al S) y Centro Ibérica (al N). Dentro de esta zona de cizalla afloran rocas de la Serie Negra que contienen oro; se trata de unidades esencialmente metasedimentarias con esquistos, cuarcitas, areniscas y calizas, con intercalaciones de anfibolitas y rocas volcánicas félsicas. Las cuarcitas negras, características de esta serie, muestran una importante recristalización, a menudo con extinción ondulante y microestilolitos; además, la presencia de golfos de corrosión y caras cristalinas irregulares ponen de manifiesto la historia tectónica del lugar. Su color oscuro se debe probablemente a la inclusión de láminas de espesor micrométrico ricas en C. Aunque previamente fueron clasificados como cherts, las evidencias apuntan a que su fuente más probable esté relacionada con detritos de rocas sedimentarias ricas en cuarzo, en concordancia con las características geoquímicas de un protolito sedimentario rico en cuarzo. Sus características geoquímicas también sugieren que pudieron generarse en un contexto de margen pasivo; no obstante, algunas muestras parecen sugerir su relación con un paleoarco volcánico oceánico a continental, conforme con los valores de las razones Th / Sc y La / Th, que apuntan a una composición de carácter intermedia para el protolito, lo que es corroborado mineralógicamente.*

Palabras clave: *Zona de Cizalla, Coimbra-Córdoba, Serie Negra, cuarzita negra.*

Oliveira, D.P.S., Silva, T.P. and Guimaraes, F. (2016): Mineralogical and geochemical characterization of Série Negra black quartzites, Coimbra-Cordoba Shear Zone, East Portugal. *Revista de la Sociedad Geológica de España*, 29(2): 23-38.

The Coimbra-Cordoba Shear Zone (CCSZ) occurs at the boundary that separates two distinct tectonostratigraphic areas of the Iberian Massif, the Ossa Morena and Central Iberian Zones in the south and north, respectively (Burg et al., 1981).

Within the CCSZ [also known as the Badajoz-Cordoba Shear Zone (Ábalos *et al*., 1991)], or the Central Unit (Azor et al., 1994), outcrop several lens-shaped, dark or black, silicified units (Fig. 1), which are typical of the Série Negra (Black Series) metasedimentary succession (Fig. 2). Over the last decades, these units have been referred to a variety of terms that includes metacherts, (meta)lydites, phthanites (siliceous shales) and quartzites in the literature (e.g. Gonçalves, 1971; Gonçalves and Fernandes, 1973; Gonçalves et al., 1971, 1972a, 1972b, 1978; Ábalos and Eguiluz, 1989; Gonçalves and Carvalhosa, 1994; Pereira, 1995, 1999; Pereira and Silva, 2000; Bandres et al., 2002, among others). This range of terminology which links these rocks to a particular environment and mode of deposition has been brought about by the ambiguous appearance of these black silicified units in the field, which vary from very fine-grained rocks to medium- to coarse-grained rocks.

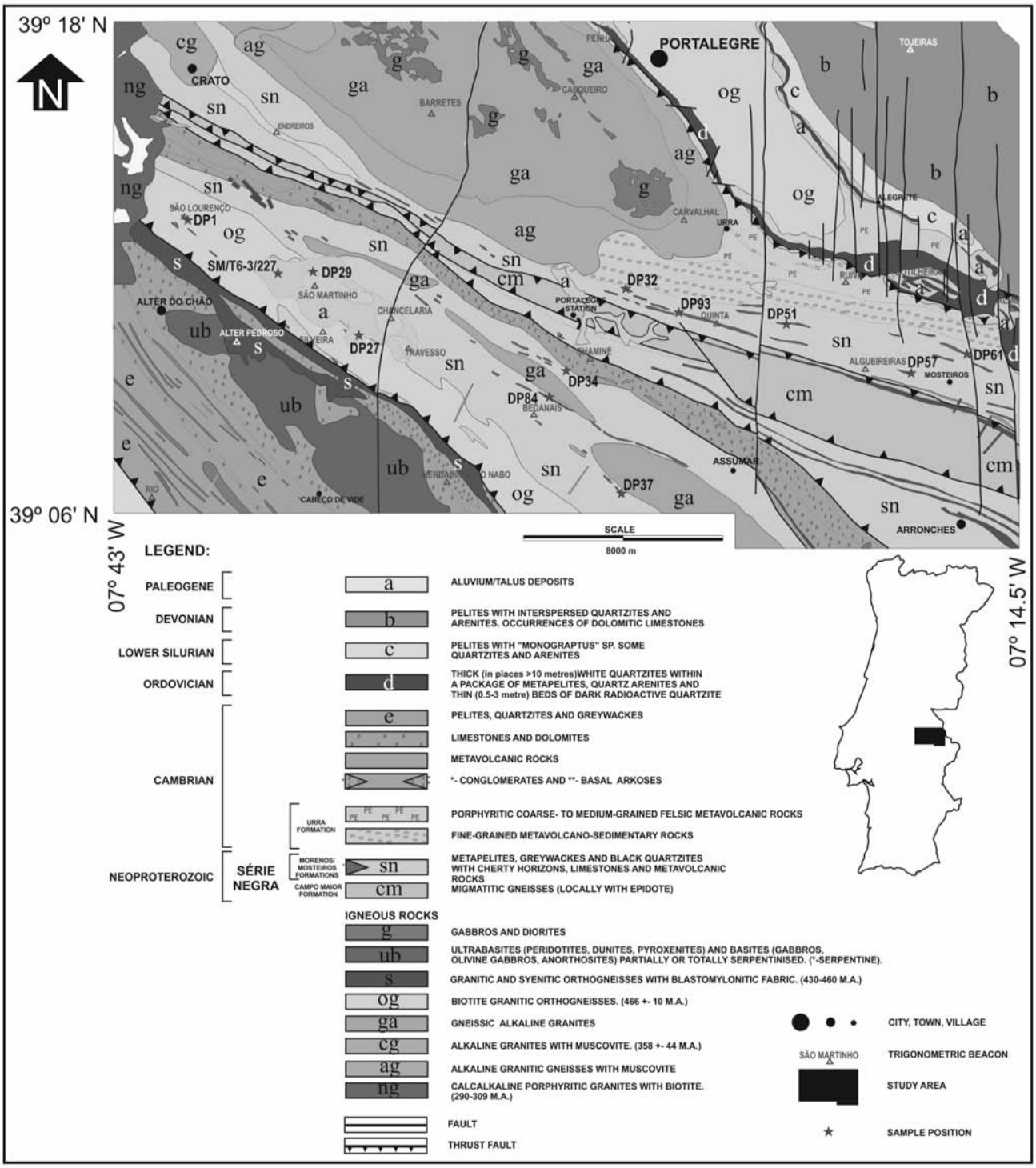

Fig. 1.- Simplified geological map of the studied area and sample location points within the Coimbra-Cordoba Shear Zone. Adapted after Gonçalves et al. (1971, 1972b), de Oliveira (2001) and Díez Fernández et al. (2014).

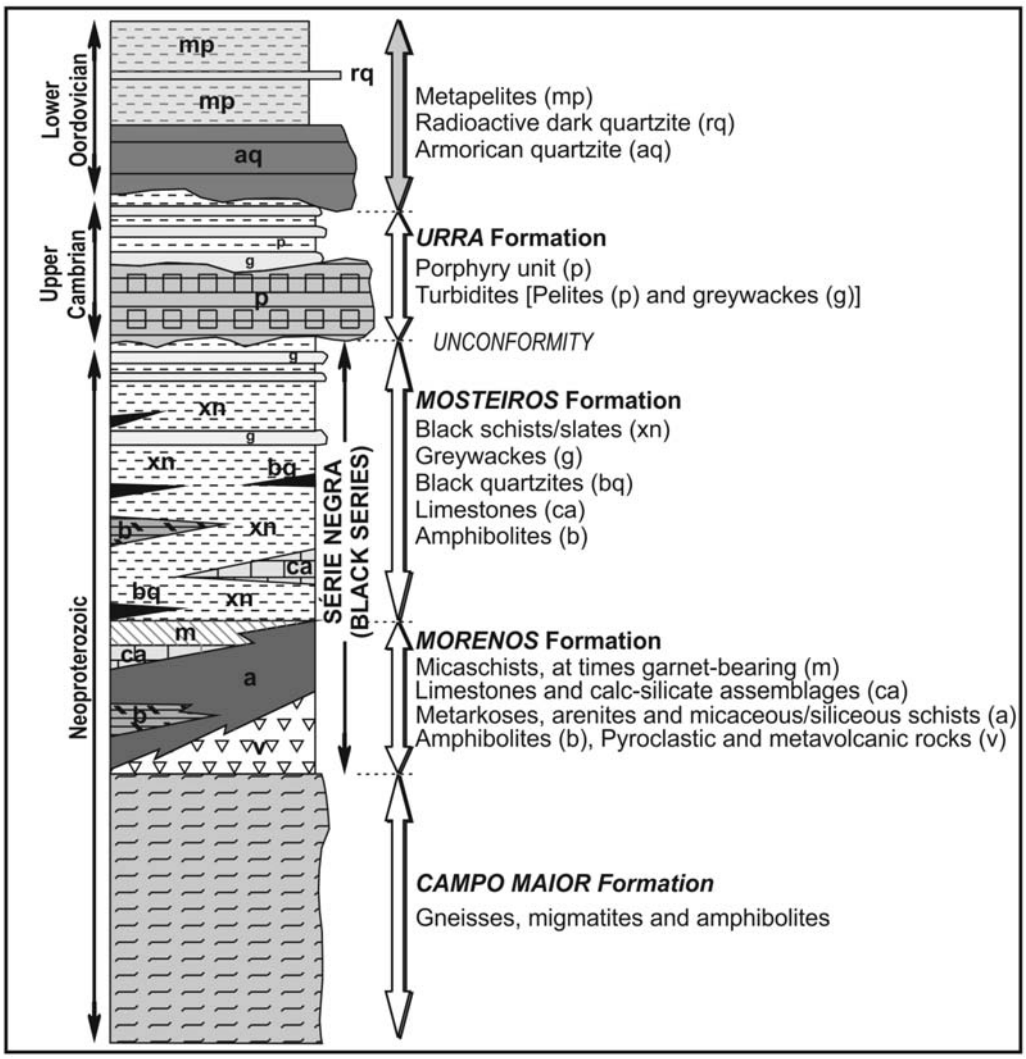

Fig. 2.- Schematic and idealized stratigraphic sequence for the Série Negra and adjacent rocks within the studied area. Adapted after Oliveira et al. (1991).

In a general way, these type of rocks are very hard and resistant to weathering making them a useful building stone in rural settings due to their regular dark colors and anti-slip characteristics. In addition, these particular rocks outcrop in economically important areas due to its hosting significant cross-border gold mineralization (de Oliveira, 2001; de Oliveira et al., 2007).

The chosen nomenclature implies the difference between chemical and clastic sedimentation processes and, ultimately, whether these have been correctly applied to the rocks in question. Due to the persistence of the terms metachert, (meta)lydite, phthanite and quartzite in the literature and following preliminary studies (de Oliveira et al., 2003a, 2003b), the purpose of this paper is to provide mineralogical and geochemical evidence of the environments of deposition and tectonic history that these rocks have undergone, an important factor for correctly naming the type of protolith and their implied geotectonic setting.

Geological setting

The CCSZ represents a major shear zone of the European Variscan orogen and is geologically complex and diverse, showing intense deformation and metamorphism contemporaneous with a large sinistral displacement, which may be due to a large intracontinental sinistral fault active during the Variscan Orogeny (Berthé et al., 1979) with displacements of 100 km (Burg et al., 1981) to 300 km (Ábalos and Eguiluz, 1992). The boundary set by the CCSZ (Burg et al., 1981) is a 600 km-long Variscan metamorphic belt with high-pressure rocks (granulites and eclogites; Eguiluz et al., 1990; Azor et al., 1994; Pereira et al., 2008, 2010; Diéz Fernández et al., 2014). This shear zone has been interpreted as either a Neoproterozoic (Cadomian) suture reworked during the Variscan cycle (Ábalos et al., 1991; Quesada, 1991; Eguiluz et al., 2000), or a Variscan suture resulting from a possible closure of an early Paleozoic ocean (Azor et al., 1994; Ordóñez Casado, 1998; Gómez-Pugnaire et al., 2003; Simancas et al., 2005), or appears to represent a major intra-continental shear zone connected in some way to the Variscan suture zone (Pereira et al., 2010).

The Série Negra occurs juxtaposed on both the north and south limbs of the CCSZ suture, which contains, from north to south, low-grade metamorphic rocks (greenschist facies) to intermediate-grade metamorphic rocks (amphibolite facies) separated by a central corridor of Neoproterozoic high-grade metamorphic rocks (blastomylonites). The Portuguese sector of the CCSZ comprises a series of fault-separated, polymetamorphic structural-tectonic subdomains where the Neoproterozoic Série Negra rocks crop out.

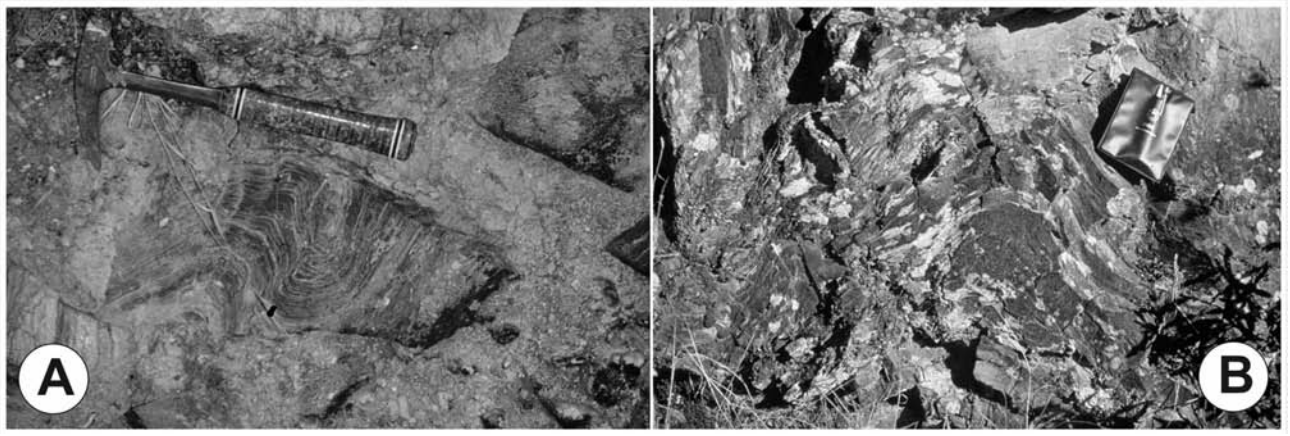

Fig. 3.- Outcrops of black quartzite within the study area. **A:** Site of sample DP93; **B:** Site of sample DP57.

The Série Negra (Black Serie) is a sequence of Neoproterozoic metasediments (Cadomian basement) consisting of siliciclastic (metagreywakes and metapelites), basic igneous (amphibolites and banded amphibolites) and felsic volcanic (metarhyolites) rocks and few limestones levels (Fig. 2; e.g. Oliveira et al., 1991; de Oliveira, 2001).

The maximum depositional age for the sedimentation have been documented ca. 590–545 Ma (e.g., Schäfer et al., 1993; Ordoñez-Casado, 1998; Eguiluz et al., 2000; Linnemann et al., 2008).

Stratigraphically, the Série Negra comprises the (lower) Morenos and (upper) Mosteiros Formations (Fig. 2). The Morenos Formation is made up of micaceous schists that are locally garnet-bearing, limestones and calc-silicate rocks, meta-arkoses, meta-arenites (quartzites) and micaceous and siliceous schists, amphibolites and metapyroclastic rocks. The Mosteiros Formation consists of black schists/slates, greywackes, black quartzites, limestones and amphibolites. North of the central corridor of high-grade metamorphic rocks and unconformably overlying the Mosteiros Formation occurs the Urra Formation that includes a lower porphyry unit and an upper pelite/greywacke unit (Oliveira et al., 1991) of Upper Cambrian-Lower Ordovician age (Solá et al., 2008). At the CCSZ boundaries, a (Lower) Cambrian sequence of platform sediments is preserved, which unconformably overlies the Neoproterozoic Série Negra metasediments and consists of micaceous schists, amphibolites, metamorphosed carbonate rocks and pelitic schists (Oliveira et al., 1991; Pereira, 1995).

The black quartzites of the Série Negra crop out in relatively short, ribbon-like (lens-shaped) outcrops which trend NW-SE (Fig. 1), parallel to the regional foliation. Outcrops are generally narrow and short (2-3 m wide and 5-10 m long, respectively) but can be several hundreds of meters long and up to 60-80 m high above the surrounding Alentejo plain. Generally, outcrops are aligned with each other defining one or several "belts" or levels. Grain size varies from outcrop to outcrop but invariably most are very fine-grained (frequent) to medium-grained (rare), highly siliceous and resistant to weathering and breakage. In some instances, these outcrops exhibit marked folding (Fig. 3). These rocks appear homogeneous in some outcrops although in others there is a manifest inhomogeneity that defines centimeter-scale layering that may represent relict bedding (de Oliveira, 2001). The quartzites are closely associated with prominent gold prospects (de Oliveira, 2001; de Oliveira et al., 2007).

Materials and methods

Within the study area, a total of twelve samples of quartzites were collected for the geochemical and mineralogical study (see location of samples in Fig. 1), all of them with a dark grayish color in hand specimen with the exception of samples DP29 and T6/3/227 that were classified as pale quartzites. The latter are almost white/beige or slightly grayish. All samples were collected in outcrops apart from sample T6/3/227 that was collected in an exploration trench. Enough material was collected to allow for milling and thin section preparation. The remainder of the samples was archived.

Major and trace elements of rock samples were analyzed by X-ray fluorescence (XRF) at the Department of Geology of the Witwatersrand University (RSA) and at the Activation Laboratories (Canada) using instrumental neutron activation analysis (INAA), inductively coupled plasma (ICP), and infra-red (IR) analytical methodologies. Quality control was assured by internal protocols at the laboratory (see www.actlabs.com).

Polished sections of quartzite samples were first studied in transmitted and reflected light under the optical microscope (Olympus BX60). In order to complement the petrographic studies, the identification of crystalline components was achieved through a Philips PW 1500 powder diffractometer with Bragg-Brentano geometry equipped with a large-anode copper tube operating at 50 kV-40 mA and a graphite crystal monochromator, to collect X-ray diffraction (XRD) patterns of the bulk powdered samples at LNEG. The quartzites were also observed using a stereomicroscope (Zeiss, Stemi SV-11) and images of the granulometric fractions < and >200 mesh (75 μm) were collected with a digital camera Zeiss (AxioCam MRc).

Selected samples were also analyzed using a JEOL JXA-8500F microprobe operating at 15kV in the Mineral Science and Technology Unit. In this study, EDS spectra and back scattered images were obtained. Natural compounds, minerals and synthetic standards were used for quantitative analysis: albite (Na), apatite (P, Ca), almandine (Al), pyrite (S, Fe), $MnTiO_3$ (Mn, Ti), olivine (Mg), orthoclase (Si, K), barite (Ba).

Results

Petrography and mineralogy

These rocks are characteristically matrix-poor. There is very little in the way of inter crystal matrix material such as a pronounced clay fraction. In all samples studied the petrographic observation shows that the main component of these rocks, quartz, is strongly recrystallized. This recrystallization is apparent in the crystal boundaries with 120º faces and embayed and irregular crystal faces (Figs. 4A and B). The quartz grains also register the effects of the tectonic history on these rocks often exhibiting undulose extinction (Fig. 4B) and microstylolites.

Previous studies of these rocks (de Oliveira et al., 2003b) have already shown to contain quartz grains that

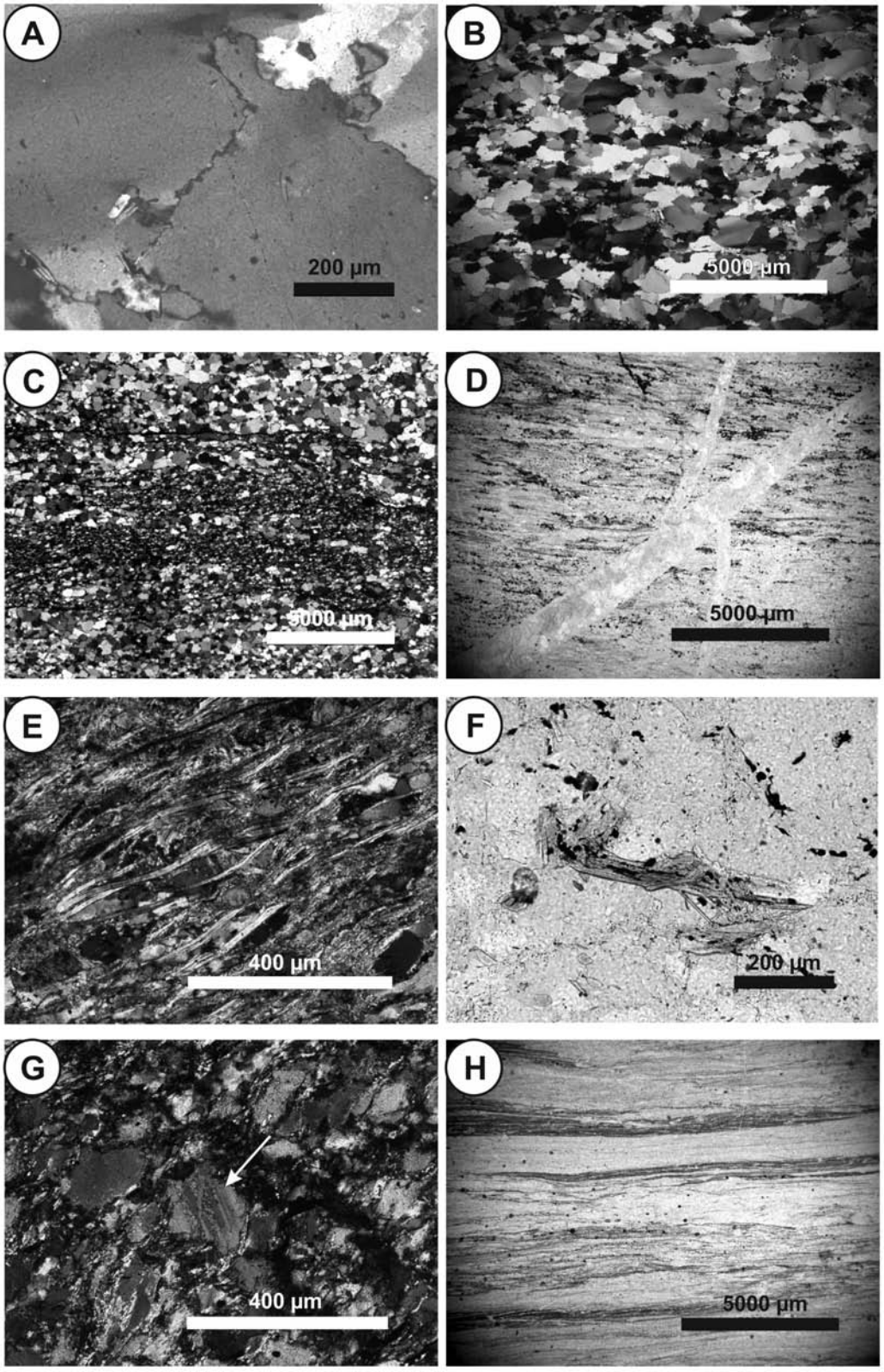

Fig. 4.- General aspects of the transmitted light petrography of the samples collected for this study. **A:** Evidence of grain recrystallization with very irregular crystal boundaries with 120º faces and embayed and irregular crystal faces (cross polarized light, 5X, sample DP27); **B:** Anhedral quartz crystals with undulose extinction (cross polarized light, 5X, sample DP57); **C:** Interlayered coarser- and finer-grained quartz layers evidencing relict bedding (cross polarized light, 5X, sample DP51); **D:** Two generations of later microveinlets in black quartzite. (plane polarized light, 5X, sample DP32); **E:** Interstitial orientated muscovite/biotite (cross polarized light, 20X, sample DP34); **F:** Grain of biotite mica altering to chlorite in sample DP27 (plane polarized light, 40X); **G:** Subhedral plagioclase crystal in sample DP61 (cross polarized light, 20X); **H:** relict, very fine bedding (S_0) in sample DP93 (plane polarized light, 1.25X).

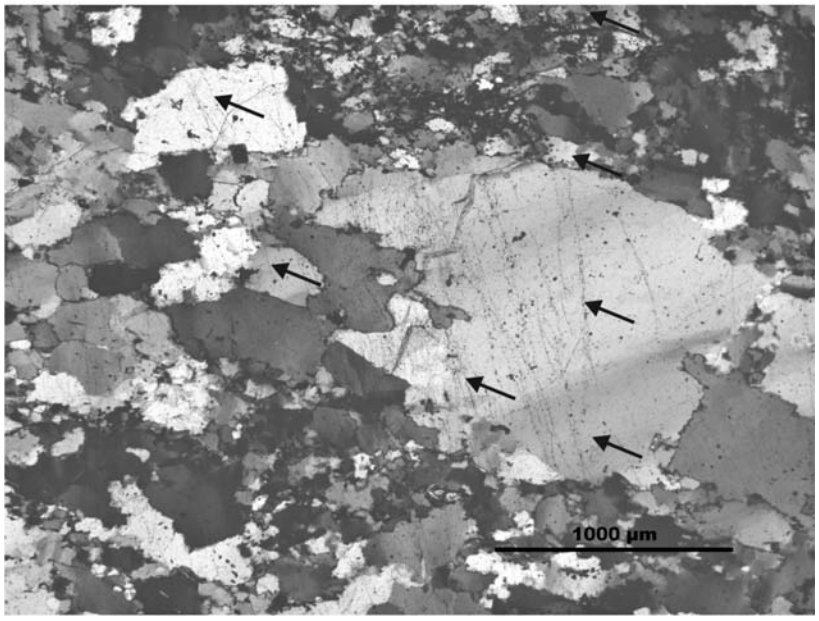

Fig. 5.- Sample DP27 showing long, continuous fluid inclusion planes (arrows) across several grain boundaries.

vary in size from 6 to 63 µm in fine-grained samples and from 30 to 600 µm in coarse-grained samples. Most samples collected can be classified as fine-grained with the exception of DP27, DP34 and T6/3/227. However, quartz grain size is also inhomogeneous: the same sample can have both layers that are finer grained and adjacent layers that are coarser grained as in sample DP51 (Fig. 4C) showing preserved relict bedding. Samples are also often cross cut by later quartz veins (Fig. 4D). De Oliveira (2001) indicates at least 3 generations of distinct quartz veins. Besides quartz, the black (and pale) quartzites contain accessory graphite, biotite/muscovite ± chlorite (Figs. 4E and F) ± rutile ± plagioclase (very rare; Fig. 4G). In the coarse-grained samples accessory biotite (± chlorite) is found interstitially to quartz and at times aligned according to the regional schistosity (NW-SE). Graphite is particularly well represented in sample DP93. Additionally there are blue-grey bands made up of heavy minerals (Fig. 4H) visible at low magnifications (5x/10x), that seems to mark bedding planes (S_0). The heavy minerals are observed in wafers, up to 200 µm thick, as dark streaks/bands across the samples. These same bands are almost invisible at higher magnifications. The opaque mineralogy of these rocks include euhedral pyrite with traces of chalcopyrite, euhedral pyrite with magnetite inclusions (magmatic origin?), rutile, Fe-oxides, marcasite (after pyrrhotite) and euhedral arsenopyrite crystals. Often the pyrite is altered to oxy-hydroxides. In addition, rare, discrete sub-rounded grains of magnetite (at times with nuclei of spinel), chromite and ilmenite have been observed (cf. Fig. 3 in de Oliveira et al., 2003b). These are larger than the host quartz.

Another aspect that the petrography study has highlighted is the presence of very long and continuous fluid inclusion planes (FIP). These are invariably composed of stretched and necked fluid single phase (only fluid) and two-phase fluid inclusions (fluid + gas) that continue uninterrupted across many different grains (Fig. 5). Their present morphology precludes them from being suitable for obtaining microthermometric data.

Corroboration of the mineralogy identified under the polarizing microscope was done using X-ray diffraction (XRD). The mineralogical characterization is summarized in Table I and Fig. 6.

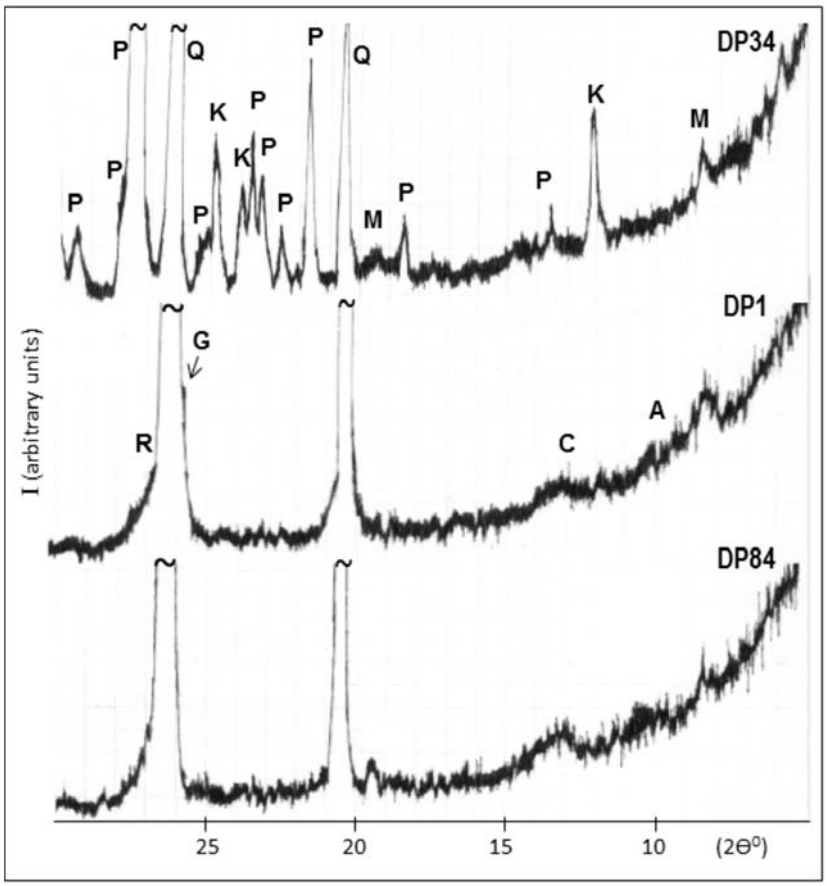

Fig. 6.- X-ray diffraction (XRD) patterns (Cu Kα radiation) of representative samples. Main identified crystalline phases: A – Amphibole, C – Chlorite, G – Graphite, K – Kaolinite, M – Mica, P – Plagioclase, Q – Quartz, R – Rutile.

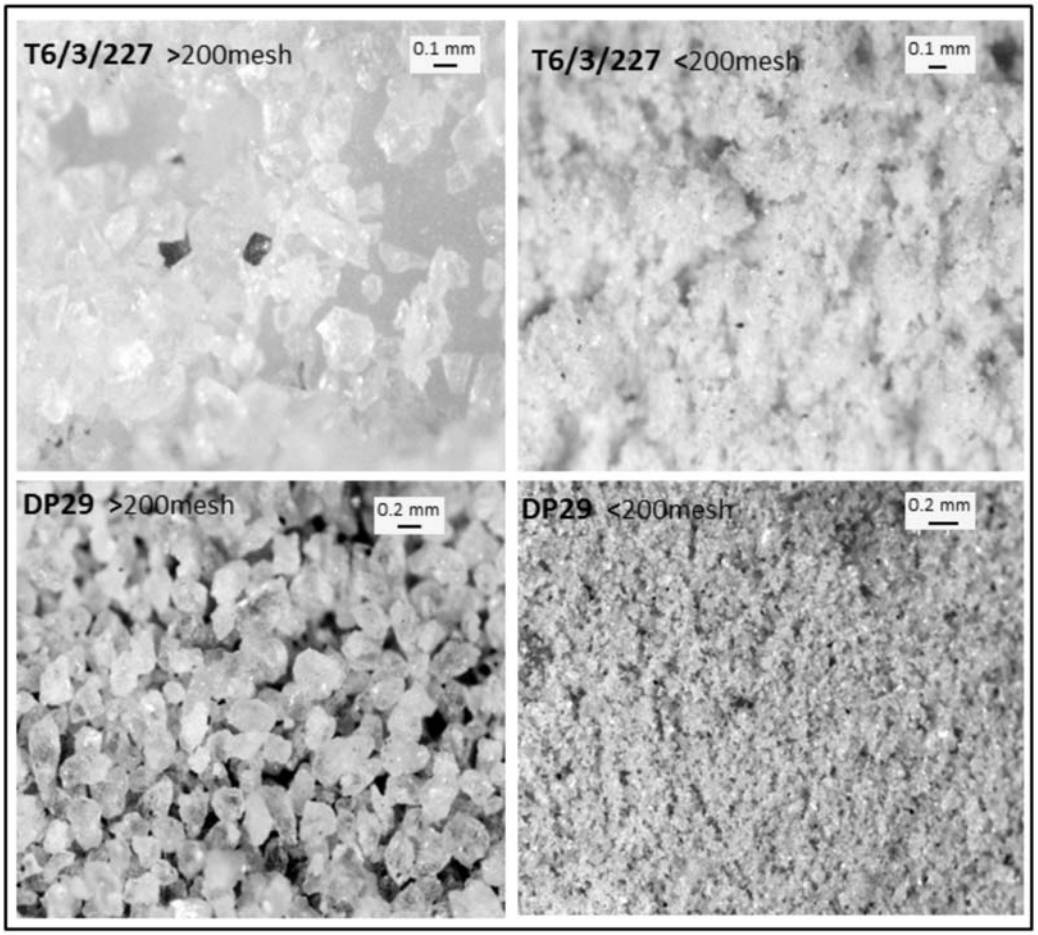

Fig. 7.- Stereomicroscope images collected from pale quartzites (light-brown disaggregate samples).

Quartz is the most abundant mineral in the studied rocks as was observed through petrography. Chlorite is present in all samples as well as rutile (with the exception of DP34 and 57, where the main line of quartz and plagioclase hinder the presence of rutile). Broad lines at *d* (inter-planar distances) values of about 8.4 and 7 Å were attributed respectively to amphibole and chlorite, while the line at about 10 Å was assigned for mica. Graphite was identified with some doubts due to the overlay with the main line of quartz. Other minerals like kaolinite and vestigial chromite plus arsenopyrite were occasionally assigned.

Sample Ref.	Color	Phases identified Main	(JCPDF card quoted bellow) Minor / Vestigial
DP1	Brownish	Qz	C + M + R + A + G + Cr?
DP27	Light-gray	Qz	C + M + R + G + Ars?
DP32	Brownish	Qz	C + M + R
DP34	Dark gray	Qz + P + K	M + C? + G?
DP37	Brownish	Qz	C + M + R + Cr?
DP51	Dark gray	Qz	C + M + R + G
DP57	Brown-grayish	Qz	C + M + P + A
DP61	Light-gray	Qz	C + M + R + A + P?
DP84	Brownish	Qz	C + M + R + A
DP93	Very dark gray	Qz	C + M + R + G
DP29	Light-brown	Qz	C + M + R + A
T6/3/227	Light-brown	Qz	C + R

Ars – Arsenopyrite, FeAsS (PDF #014-0218); Cr – Chromite, Fe(Cr,Al)2O4 (PDF #003-0873); G – Graphite, C (PDF #023-0064);
K – Kaolinite, Al2Si2O5(OH)4 (PDF #014-0164); Qz – Quartz, α-SiO2 (PDF #005-0490);
R – Rutile, TiO2 (PDF #004-0551). A – Amphibole; C – Chlorite; M – Mica; P – Plagioclase.

Table I.- XRD mineralogical characterization of powdered quartzite samples.

Previously, the dark color of these rocks has been attributed to the presence of iron oxides, carbon or graphite (e.g. Ábalos and Eguiluz, 1989; Jödicke et al., 2007; Puelles et al., 2013, 2014). However, no correlation was found between the chemical analyses (namely carbon and iron contents) or mineralogical phases (graphite) and the dark color of quartzites in the present study (see Tables I and II). The disaggregation of grayish hand samples giving rise to little sand-like grains, revealed interesting aspects exemplified in Figs. 7-9. Rare black particles were observed with quartz grains in pale quartzites (light-brown disaggregate samples, Fig. 7). Darker grayish samples (Fig. 8) have more black particles mixed with the minerals. Sample DP93 is the darkest of the group both in hand specimen and after the disaggregation, where layers of black particles were observed (Fig. 9) in quartz grains. A previous Raman study (de Oliveira, et al., 2003b) conclusively identified amorphous carbon in these layers. However, it seems that the gray color of the rock is a global effect due to the dissemination and quantity of black/dark particles (including C-flakes) in relation to light-colored or transparent minerals, namely quartz.

Both energy and wavelength dispersive microprobe analyses of sample DP93, the darkest sample of all, both

	Anal. met.	Det. limit	Unit symb.	DP1	DP27	DP32	DP34	DP37	DP51	DP57	DP61	DP84	DP93	DP29	T6/3/227
SiO2	XRF	0.10	%	92.69	96.44	99.37	62.93	97.84	100.62	90.06	72.75	87.93	73.93	98.08	98.48
TiO2	"	0.01	%	0.31	0.28	0.23	0.94	0.30	0.09	0.20	0.67	0.28	0.76	0.26	0.22
Al2O3	"	0.10	%	5.31	1.02	0.52	16.83	1.10	0.55	6.21	15.69	5.58	13.02	0.65	0.87
Fe2O3	"	0.01	%	0.94	1.11	0.49	6.63	0.99	0.36	1.25	4.69	1.98	5.62	0.60	0.84
MnO	"	0.01	%	0.01	bd	0.01	0.05	bd	0.04	0.04	0.05	0.04	0.03	bd	bd
MgO	"	0.01	%	0.34	0.11	0.01	2.98	0.17	0.23	0.43	1.50	0.50	2.14	bd	0.02
CaO	"	0.01	%	0.10	0.10	0.10	1.63	0.18	0.04	0.11	0.15	0.08	0.22	0.08	0.07
Na2O	"	0.01	%	bd	0.02	0.03	2.58	0.08	bd	0.83	bd	1.70	bd	bd	0.10
K2O	"	0.01	%	0.11	0.24	0.08	2.83	0.26	bd	0.64	2.77	1.13	2.09	0.09	0.01
P2O5	"	0.01	%	0.03	0.04	0.02	0.23	0.09	0.19	0.06	0.09	0.09	0.20	0.12	0.03
LOI			%	1.45	1.25	0.52	2.35	0.59	0.41	0.44	0.42	1.30	0.53	0.51	0.28
TOTAL			%	101.31	100.63	101.38	99.99	101.61	102.53	100.28	98.79	100.60	98.54	100.41	100.93
Cr	"	9	ppm	500	513	247	141	504	108	247	89	352	13	306	393
Ba	"	5	ppm	513	1279	50	565	1687	165	72	62	1096	216	286	47
Rb	"	3	ppm	bd	bd	bd	89	bd	bd	5	bd	42	bd	bd	bd
Y	"	3	ppm	32	39	bd	21	85	4	5	4	35	4	11	bd
Zr	"	6	ppm	19	26	20	169	32	17	21	27	105	21	21	14
Nb	"	3	ppm	6	13	6	17	7	6	7	5	9	7	6	7
Au	INAA	2	ppm	19	320	16	21	17	3	5	7	18	6	18	19
As	"	0.5	ppm	15	190	85	2.9	9.3	4.6	5.7	2.9	15	8.6	15	47
Sb	"	0.1	ppm	3.3	1.4	2.1	0.5	2	0.7	1	1.2	1.1	4	2.3	0.4
Sc	"	0.1	ppm	1.4	1.3	14	1.4	7.2	2.3	2	4.2	2.8	29	0.9	2.7
Th	"	0.2	ppm	0.4	0.9	0.3	7.5	0.8	0.3	0.9	0.3	3.7	0.4	0.6	3.5
U	"	0.5	ppm	9	50	0.6	2.1	7.4	0.9	bd	0.7	8.5	0.9	9	1.2
La	"	0.5	ppm	10	17	1	21	19	18	5.5	1.4	20	1.9	4.5	7.6
Ce	"	3	ppm	7	12	bd	40	24	62	15	4	29	5	5	12
Nd	"	5	ppm	13	19	bd	14	22	23	8	bd	19	bd	8	9
Sm	"	0.1	ppm	2.3	3.3	0.4	3	4.4	5.2	1.6	0.4	3.6	0.7	1.1	1.8
Eu	"	0.2	ppm	0.7	1.2	bd	1.2	1.5	1.6	0.4	bd	1.1	0.2	0.3	0.5
Tb	"	0.5	ppm	0.6	0.6	bd	bd	1.2	0.6	bd	bd	0.8	bd	bd	bd
Yb	"	0.2	ppm	2.9	3	0.5	2.7	6.4	0.5	0.6	0.6	3.2	0.8	1.2	2.3
Lu	"	0.05	ppm	0.44	0.43	0.08	0.43	0.94	0.09	0.1	0.09	0.49	0.13	0.18	0.34
Mo	ICP	2	ppm	5	12	2	bd	bd	bd	bd	bd	2	4	8	bd
Cu	"	1	ppm	39	41	6	11	21	6	10	4	33	16	15	6
Pb	"	4	ppm	9	13	bd	10	41	bd	6	bd	29	bd	19	5
Zn	"	1	ppm	33	38	6	47	76	3	8	4	40	9	8	2
Ag	"	0.4	ppm	0.6	1.5	bd	bd	0.9	bd	bd	bd	bd	bd	0.5	bd
Ni	"	1	ppm	1330	1412	1374	374	1059	504	935	342	741	898	800	2113
Sr	"	1	ppm	4	20	5	201	21	46	16	2	57	3	8	7
V	"	2	ppm	659	1856	7	110	387	9	16	10	537	23	298	8
C	IR	0.01	%	1.25	1.21	0.45	0.18	0.36	0.22	0.09	0.2	0.37	0.47	0.32	0.05

Table II.- Analytical data set of the Série Negra rocks (XRF: X-ray fluorescence; INAA: instrumental neutron activation analysis; ICP: inductively coupled plasma; IR: infra-red; LOI: loss on ignition; bd: below detection limit).

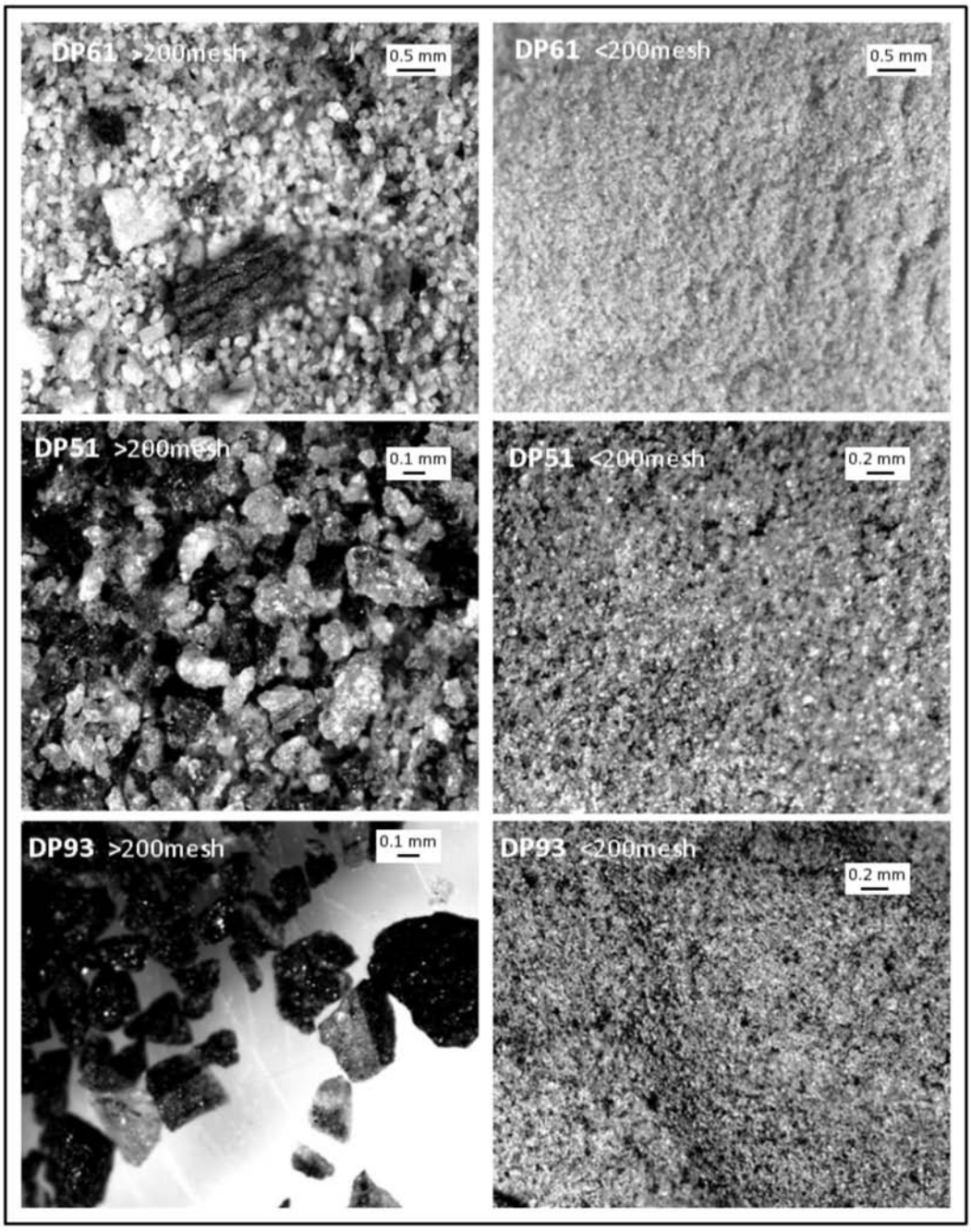

Fig. 8.- Stereomicroscope images of grayish (darkest) quartzites.

in hand specimen and under the microscope, revealed that the majority of the constituent minerals were quartz (silicon 38.52%) with traces of barium (0.62%), titanium (0.14%), iron (0.17%), magnesium (0.66%), manganese (0.01%), aluminum (5.63%), potassium (2.35%), sodium (0.02%), phosphorus (0.02%) corroborating the bulk values shown in Table II. Additionally, there is no difference in quartz chemistry between dark and light layers in the sample (Fig. 4H). However, the darker layers appear to be more pitted than the light areas. The individual darker points visible under thin section and analysed at the microprobe indicated that these "spots" are richer in carbon than the adjacent quartz grains (Fig. 10). These features are not uncommon in other rocks with similar characteristics, for example Krabbendam et al. (2003) and Sugahara et al. (2010).

Geochemistry of quartzites

Table II presents the results of chemical analyses obtained for the Série Negra rocks, black plus pale (the last two samples) quartzites. All rocks present SiO_2 content higher than 60% and some of them have exclusively only silica plus minor contents of other oxides (DP27, 29, 32, 37, 51 and T6/3/227). These data are in conformity with those presented for quartzites and quartz phyllites by some authors (e.g. Aires et al., 2013; Pereira et al., 2006).

Geochemically, three groups of samples could be distinguished by analyzing Fig. 11, where the references were simplified. Sample DP34 is clearly different (Tables I and II) through the lowest content of SiO_2 and the highest level of LOI plus the other oxides, associated to the presence of plagioclase and kaolinite as the main mi-

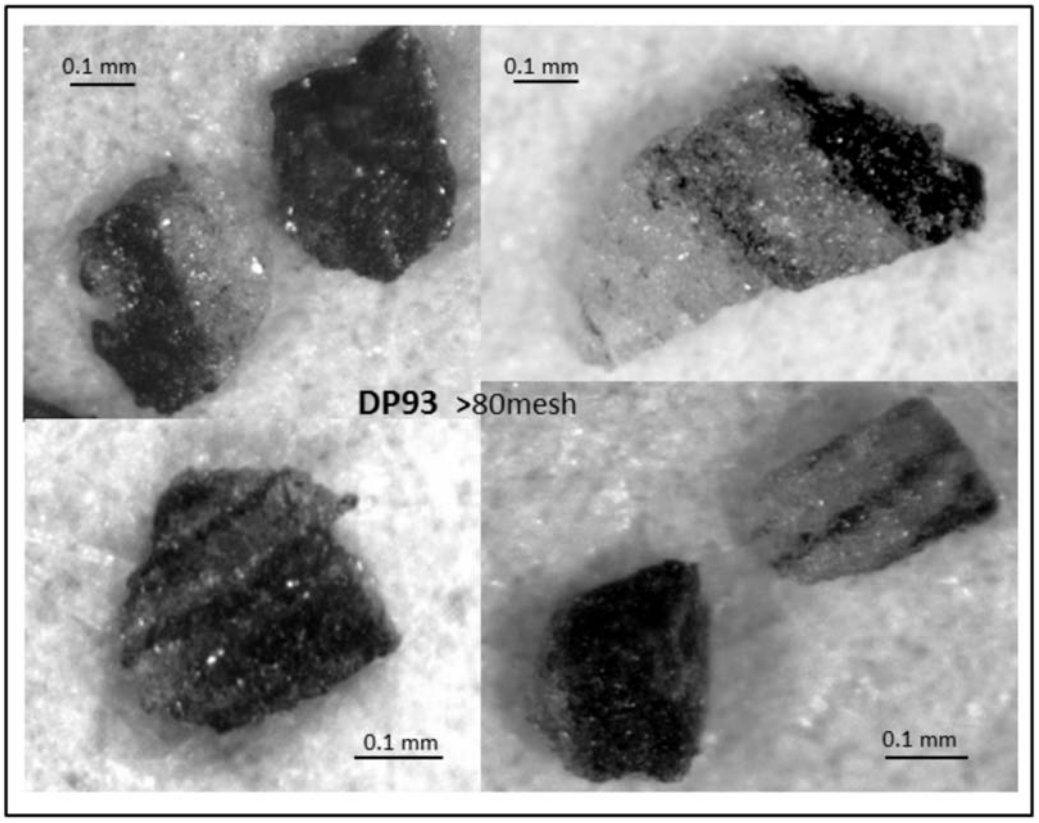

Fig. 9.- Stereomicroscope images collected from sample DP93 showing layers of black particles in quartz grains.

neralogical phases. DP61 and 93 are similar in what concern the chemical content (about 70% of SiO_2, 0.7% TiO_2, 15% Al_2O_3, 5% Fe_2O_3, 2% MgO and 2.5% K_2O), but in the first amphibole was identified while rutile is present in the second. These three samples constitute a cluster as exemplified by the graphs SiO_2 *vs* Al_2O_3, SiO_2 *vs* Fe_2O_3 and TiO_2 *vs* Al_2O_3 (Figs. 11A, B and C).

Another group is formed by the rocks with references DP1, 57 and 84, distinguishing from the others by the medium content of silica, alumina and magnesia, respectively about 90, 5.5 and 0.4%, all of them having chlorite, mica and amphibole well expressed. Plagioclase was also identified in DP57 but less represented than in sample DP34. High contents of Cr plus Ni were noticed in sample DP1, while in DP84 high levels of Ba plus Zr were detected.

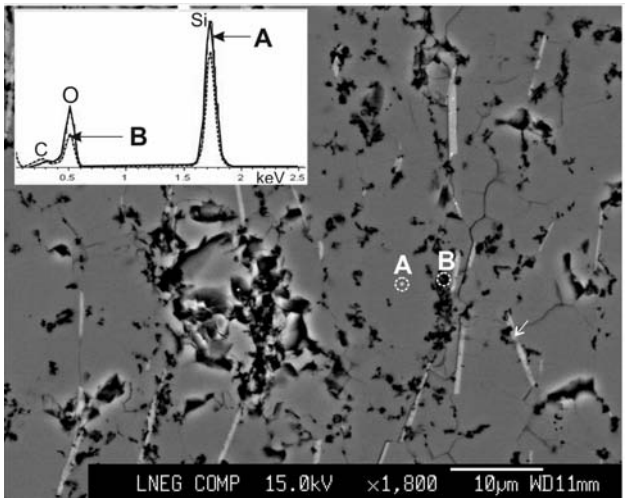

Fig. 10.- Backscattered electron image of sample DP93 showing detail of black particles within quartz grains. Circles mark the irradiated points (A- plain quartz; B- carbon rich area). Inset shows the corresponding EDS spectra. The arrow points to an area rich in barium.

The last six samples are also distinct, forming a group (Fig. 11A-C). As already mentioned, they have exclusively only silica with minor contents of other oxides (DP27, 29, 32, 37, 51 and T6/3/227). DP27 where arsenopyrite was identified (Table I), presents high contents of Cr, Ba, As, Ni and V and is the sample with the highest level of Au (320 ppm). In sample DP32 only the Ni content is significant as minor element. The sample with high content in heavy rare earth elements (REE) plus significant Cr and Ba, is DP37. The only sample where no mica was identified by XRD (T6/3/227), presents a considerable concentration of Ni.

Sediments can be classed on both textural and mineralogical maturity (Folk, 1954). In both cases, the evolution to mature sediments involves getting rid of clay minerals and retaining the dominant, resistant quartz fraction. Therefore, mineralogical maturity is best defined as a compositional state of a clastic sedimentary body wherein there is a dominance of quartz and an absence or minority of less-resistant particles such as feldspars, detrital carbonates or lithic fragments (Muhs, 2004). The composition and texture of grains in these rocks point to the maturity of the sediments (SiO_2 > 60%; the majority of samples being above 80%) as illustrated in Figs. 11A and 11B. However, a different evolution pattern is noticed in terms of textural maturity and mine-

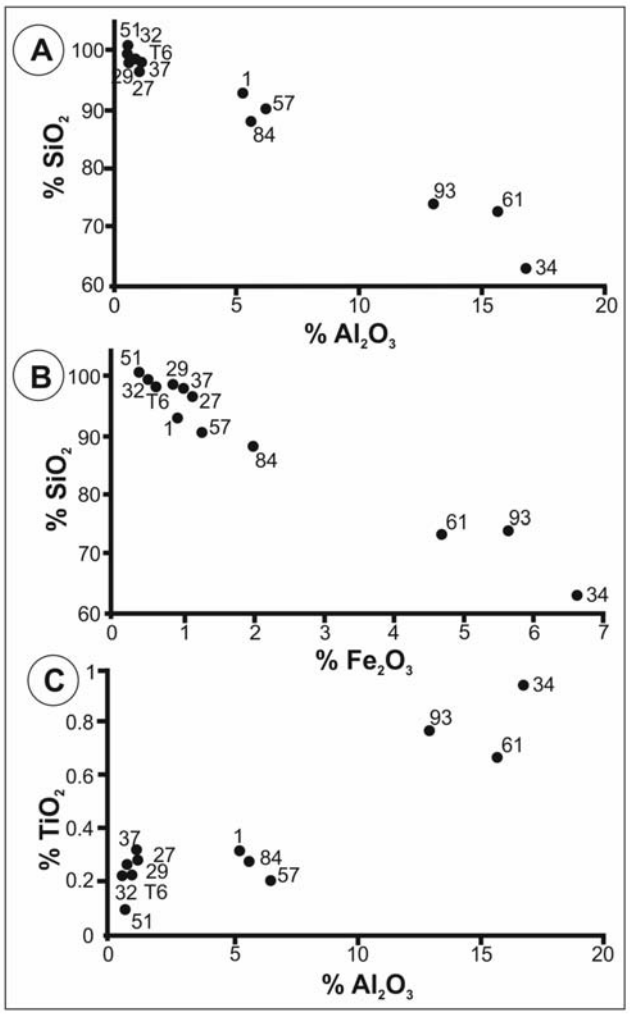

Fig. 11.- A: Graph of SiO_2 versus Al_2O_3 for the studied quartzites; **B:** SiO_2 – Fe_2O_3 variation graph; **C:** Graph of TiO_2 versus Al_2O_3 (all sample references simplified).

ralogical differentiation: DP27, 29, 32, 37, 51 plus T6/3/227 samples are the most mature and the most evolved and DP34, 61 plus 93 are the lesser ones. Between these two extreme groups lie the samples DP1, 57 and 84 closer on mineralogical differentiation and textural maturity to the "DP27 group". Fig. 6C shows the enrichment in Al_2O_3 and TiO_2 from "DP27 group" to "DP34 group" related to the amount of matrix, which is poor in "DP27 group" and more abundant in "DP34 group", probable to rutile being associated with chlorite/mica matrix.

Discussion

Relative enrichments in Ni, Co, Cr and depletion of High Field Strength Elements (HFSE) in these rocks, e.g. Th, Zr, U, may reflect absence of significant recycling of sediments (Boryta and Condie, 1990). Recycling would increase the proportion of HFSE-bearing detrital phases, *e.g.* zircon.

REE tend to increase with Al_2O_3 suggesting these elements were housed primarily in micas (originally clays?) due to the rare occurrence of plagioclase in most cases. Both sets of samples show negative Eu anomalies with the pale quartzites all falling in the middle of the black quartzite sample population. The negative Eu anomaly in Fig. 12 may show that no metamorphic feldspars were included in these samples.

The possible provenance of the material to form these protosediments could be from a granite. Comparison of the general trends and slopes obtained in most cases excludes this possibility (e.g. Boryta and Condie, 1990; McLennan et al., 1993). Further evidence may be derived from Table III that shows the La/Th and Th/Sc ratios for common igneous rocks. Geochemically, the black quartzites show Th/Sc ratios indicative of a probable provenance from a basalt, alkali basalt or andesite, *i.e*. a basic to intermediate type of volcanic rock. The pale quartzites could be derived from a granite-basalt mixture although their ratios do not correlate well with the already published data shown in Table III. When analyzing the black quartzite La/Th ratios, their values range from 3.33 to 60.00. The majority of samples show ratios around 4.5 to 6.0, which would corroborate the source being basic to intermediate. The very high La/Th ratios seem to be from samples depleted in Th. The pale quartzite shows a probable andesite-granite-basalt source although a larger sample population would be required to make these observations more statistically sound (Table III).

Mineralogical evidence complementing the fact that the possible source rocks were in fact basic to intermediate volcanic rocks is the fairly common inclusion of detrital pyrite with nuclei or inclusions of magnetite, overgrown by euhedral pyrite possibly as a result of the metamorphism. This would indicate a magmatic origin for the protosediments. However, such ratios should be interpreted in terms of provenance with care, for the ratios can be fractionated during weathering and transport and may be strictly valid for locally derived sediments. Recycled sediments and those from a mixed source are much more difficult to interpret (Rollinson, 1992) and the result presented above may be misleading as all these factors cannot be ascertained. The conflicting results may also reflect the inability of the geochemical techniques used to deal with the regional and contact metamorphic effects that have affected these rocks.

Using a modified plot (Herron, 1988) of the two index of sandstone maturity shows that the quartzite samples co-

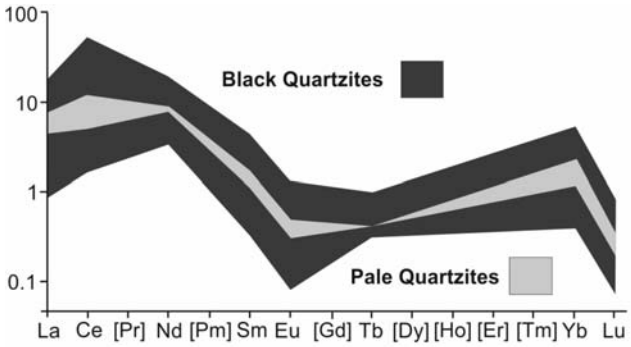

Fig. 12.- REE distribution patterns for the samples studied based on the analyses in Table II. Elements in [ ] were not analyzed. Data are normalized to average Phanerozoic quartzite.

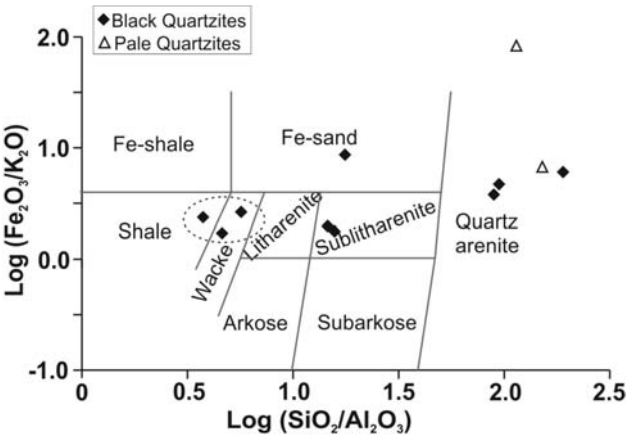

Fig. 13.- Classification diagram for terrigenous sandstones (after Herron, 1988) using the geochemical parameters of the Série Negra.

llected within the study area plot mostly in the sublitharenite and quartz arenite field (Fig. 13). However, three samples plot in the shale and wacke fields. These samples are, in a clockwise direction from left, DP34, DP93 and DP61– precisely those with highest Al_2O_3 contents (Figs. 11A and C). Results such as these would indicate that the (meta) arenites are mature sediments with sedimentary sorting having taken place to a large extent.

Unlike igneous rocks, where most discriminant diagrams are based upon trace element geochemistry, discrimination diagrams for sedimentary rocks are based on major element geochemistry and more susceptible to variations. The underlying assumption of geochemical discrimination diagrams for sedimentary rocks is that there is a close link between tectonic setting and sediment provenance. This is largely true if the sediments are immature containing a large proportion of lithic fragments from which the provenance and tectonic setting may be inferred (Rollinson, 1992). However, there is one major area of uncertainty, for some sediments are transported from their tectonic setting of origin into a sedimentary basin in a different tectonic environment (McLennan et al., 1990). Using major element geochemistry and the approach of Roser and Korsch (1988), the arenites plot in a dispersed pattern within the quartzose sedimentary provenance field (Fig. 14). These results do not contradict the previously obtained results using La/Th and Th/Sc ratios as this type of diagram is best used for greywackes.

The arenites are more mature sediments and the proportions of lithic fragments are greatly reduced. A quartz-rich source is still probable if a basic to acid rock source is taken into account. Tectonic discrimination diagrams such as those of Bhatia (1983) were used to try to determine their probable tectonic environment. One such diagram, TiO_2 *vs.* (Fe_2O_3 total + MgO) is shown in Fig. 15. Samples plot in the "passive margin", "active continental margin" and "continental arc" fields. Two samples of black quartzite also plot in the "oceanic arc" field. This conforms to results shown by Schafer et al. (1993) where the Tendudía Group (upper part of the Série Negra in SW Spain) has been interpreted to be deposited in an arc-type environment.

Série Negra rocks, including the quartzites, occur juxtaposed on both the north and south limbs of the CCSZ suture, which contains, from north to south, low-grade metamorphic rocks (greenschist facies) to intermediate-grade metamorphic

	Sample Nº	La/Th	Th/Sc	La/Th & Th/Sc values in common igneous rocks and PAAS			
Black quartzites	**DP1**	25.00	0.29	**Sample (*)**	**Lithology**	**La/Th**	**Th/Sc**
	DP27	18.89	0.69	PCC-1	Peridotite	15.0	0.001
	DP32	3.33	0.21	**BCR-1**	**Basalt**	**7.0**	**0.18**
	DP34	2.80	5.36				
	DP37	23.75	0.11	**W-1**	**Diabase**	**5.7**	**0.07**
	DP51	60.00	0.13				
	DP57	6.11	0.45	ASV-1 (1)	Andesite	7.0	0.48
	DP61	4.67	0.07	GSP-1	Granodiorite	1.9	14.79
	DP84	5.41	1.32	**G-2**	**Granite**	**2.3**	**6.49**
	DP93	**4.75**	**0.01**				
				G-1	**Granite**	**2.0**	**17.24**
Pale quartzites	**T6/3/227**	2.17	1.30				
	DP29	**7.50**	**0.66**	Ponape Island and Marquesas Archipelago (2)	Alkalic basalt	5.6 to 11.43	0.08 to 0.64
				PAAS (3)	Shale	2.6	0.91

Table III.- La/Th and Th/Sc ratios for the black and pale quartzite samples collected within the studied area. La/Th & Th/Sc in common igneous rocks compiled from Girty et al. (1993) and (*)Sources from Flanagan (1973), Dixon et al. (1984), Taylor and McLennan (1985) and Liotard et al. (1986); (1) See Gill (1981) – suggested that La/Th values for island arc andesites vary from 2.0 to 7.0; (2) range in values reported by Dixon et al. (1984) and Liotard et al. (1986) – Gill (1981) states that La/Th values in ocean island basalt vary from 7.0 to 15.0; (3) Post-Archaean average Australian shale (PAAS) in Taylor and McLennan (1985).

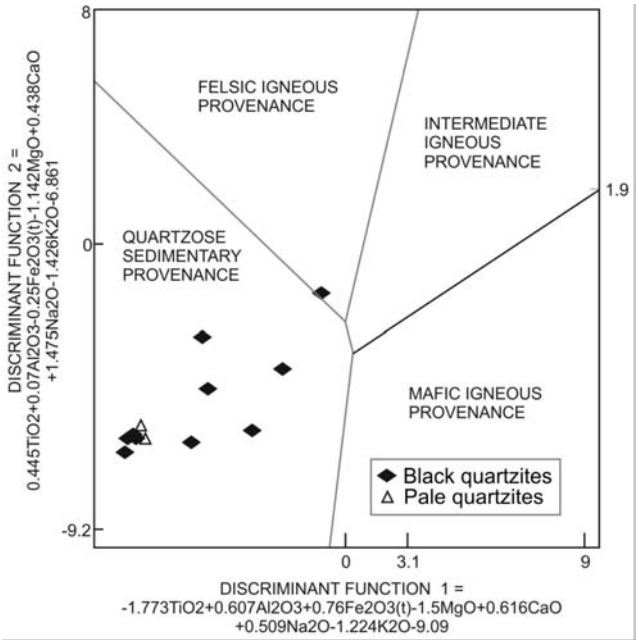

Fig. 14.- Discriminant function diagram for the provenance signatures of sandstone-mudstone suites using major element data (after Roser and Korsch, 1988). Discriminant functions calculated from values in Table II.

rocks (amphibolite facies) separated by a central corridor of Neoproterozoic high-grade metamorphic rocks (blastomylonites). The mineralogical characteristics of the Série Negra black quartzites outcropping within the CCSZ clearly show these to be recrystallized, which makes the original protolith harder to determine due to metamorphism hiding the provenance signature. Mineralogy, determined both by petrographic and diffraction methods show an extensive list of minerals or mineral phases although it is clear that these rocks are mostly made up of quartz indicating sediment maturity (SiO_2 > 60%).

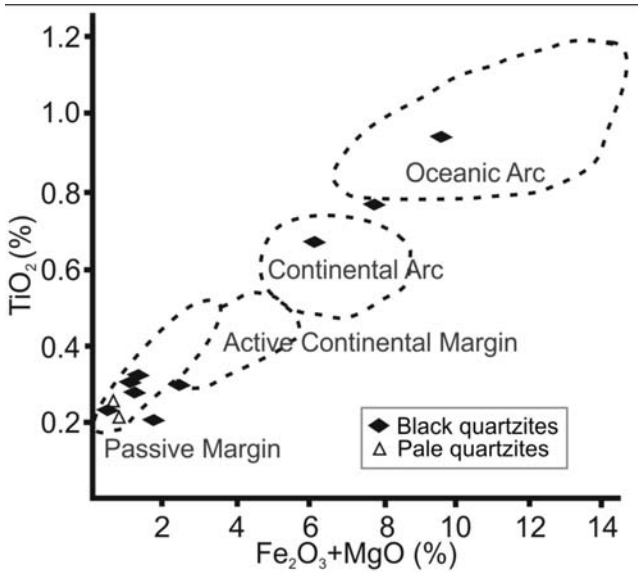

Fig. 15.- TiO_2 vs. Fe_2O_3 total + MgO discrimination diagram for sandstones (after Bhatia, 1983) for the Série Negra quartzites.

Both sandstones and cherts could be possible protoliths prior to metamorphic-induced recrystallization and field identification can induce in error due to their general cherty appearance partly in that they are mostly fine-grained with rare fine- to medium-grained facies. However, several lines of evidence point to their having a more likely detrital rather than chemical origin, namely the absence of the very thin layering or laminations commonly found in true cherts, the presence of centimetre-scale layering that probably represents relict bedding, the occurrence of subrounded (detrital) opaque minerals (magnetite, chromite and ilmenite - the latter also present as a metamorphic mineral) and the local presence of feldspar, although rare, would indicate a more arkosic precursor.

Geochemically, these samples can be split into three groups. Samples DP27, 29, 32, 37, 51 and T6/3/227 are the most mature in geochemical terms and DP34, 61 and 93 are less mature. Between these two extremes lie a "middle group" of samples, namely DP1, 57 and 84.

Protolith signatures of the source geological setting based on their geochemistry point to a quartzose sedimentary provenance and these samples plot and mostly in the quartz arenite and sublitharenite fields of the sandstone classification diagram with some variations resulting from higher Al_2O_3 contents; inferring a greater amount of feldspar, which "push" a small subset of samples (3) into the wacke field.

In terms of the paleo-geological environment, the majority of the samples' geochemistry indicates a passive margin setting although three samples tend to be spread over oceanic arc to continental arc settings.

Conclusions

In terms of the provenance of these sediments and purely from a geochemical and mineralogical point of view, the Th/Sc ratios of the black quartzites indicate a probable provenance from a basalt, alkali basalt or andesite, *i.e.* a basic to intermediate type of volcanic rock, whereas the pale quartzites seem to indicate a granite-basalt protolith mixture. The protoliths would have been derived from a probable passive margin, oceanic arc to continental arc settings.

It is undeniable that the sediments are mineralogically mature and have a quartzose sedimentary provenance plotting mostly in the quartz arenite and sublitharenite fields of the sandstone classification diagram based on their major element geochemistry.

The presence of ubiquitous carbon flakes would suggest that the characteristic dark color of these rocks is derived from the concentration of minute inclusions within the quartz grains rather than the iron oxide phases previously discussed and the fact that the carbon particles seem to be closer together in very thin layers.

Most importantly, based on the results obtained in this study and given a more probable sandstone or arenite protolith for these rocks, the correct term of *quartzite* for these rocks should be adopted definitely to describe the siliciclastic rocks of the CCSZ Black Series instead of metachert, (meta)lydite and phthanite.

Acknowledgments

This study is partially funded by BD/15877/98 awarded by the *Fundação para a Ciência e a Tecnologia*. The authors thank R. Solá for the review of the manuscript before submission. The authors also thank Juan Jiménez Millán and an anonymous reviewer for greatly improving the quality of the manuscript with their suggestions and edits. A final revision by editor Luis Miguel Nieto Albert dotted the t's and crossed the I's – thank you. Mr. Rogério Raposo is thanked for thin section preparation.

References

Ábalos, B. and Eguiluz, L. (1989): Structural analysis of deformed early lineations in black quartzites from the central Badajoz-Córdoba Shear Zone (Iberian Variscan fold belt). *Revista de la Sociedad Geológica de España*, 2: 95-102.

Ábalos, B. and Eguiluz, L. (1992): Evolución geodinámica de la zona de cizalla dúctil de Badajoz-Córdoba durante el Proterozoico Superior-Câmbrico Inferior. In: *Paleozoico Inferior de Ibero-América*, (J.C. Guttiérrez-Marco, J. Saavedra and I. Rábano, Eds.), Univ. Extremadura, 577-591.

Ábalos, B., Gil Ibarguchi, J.I. and Eguiluz, L. (1991): Cadomian subduction, collision and Variscan transpression in the Badajoz-Cordoba shear belt, southwest Spain. *Tectonophysics*, 199: 51-72.

Aires, S., Noronha, F., Carvalho, C., Moura A.C. and Ramos, J.F. (2013): The Example of the Quartzite from the "Upper Quartzite Formation" from Trás-os-Montes and Alto Douro (Northern Portugal); its characterization to use as natural stone. *Key Engineering Materials*, 548: 212-219.

Azor, A., Lodeiro, F.G. and Simancas, J.F. (1994): Tectonic evolution of the boundary between the Central Iberian and Ossa-Morena zones (Variscan belt, southwest Spain). *Tectonophysics*, 13: 45-61.

Bandres, A., Eguiluz, L., Gil Ibarguchi, J.I. and Palacios, T. (2002): Geodynamic evolution of a Cadomian arc region: the northern Ossa Morena Zone, Iberian massif. *Tectonophysics*, 352: 105-120.

Berthé, D., Choukroune, P. and Jegouzo, P. (1979): Orthogneiss, mylonite and non coaxial deformation granites: the example of the south Armorican shear zone. *Journal Structural Geology*, 1: 31-42.

Bhatia, M.R. (1983): Plate tectonics and geochemical composition of sandstones. *Journal Geology*, 91: 611-627.

Boryta, M. and Condie, K.C. (1990): Geochemistry and origin of the Archaean Beit Bridge Complex, Limpopo Belt, South Africa. *Journal Geological Society London*, 147: 229-239.

Burg, J.P., Iglesias, M., Laurent, P.H., Matte, P. and Ribeiro, A. (1981): Variscan intracontinental deformation: The Coimbra-Córdoba Shear Zone (SW Iberian Peninsula). *Tectonophysics*, 78: 61-177.

de Oliveira, D.P.S. (2001): The nature and origin of gold mineralisation in the Tomar Cordoba Shear Zone, Ossa Morena Zone, east central Portugal. Ph.D. thesis, Witwatersrand Univ., 352 p.

de Oliveira, D.P.S., Reed, R.M., Milliken, K.L., Robb, L.J., Inverno, C.M.C. and D'Orey, F.L.C. (2003a): (Meta)cherts, (meta)lydites, (meta)phthanites and quartzites of the série negra (Crato-S. Martinho), E. Portugal: towards a correct nomenclature based on mineralogy and cathodoluminescence studies. *Ciências da Terra*, nº esp. V, CD-ROM: B68-B71.

de Oliveira, D.P.S., Reed, R.M., Milliken, K.L., Robb, L.J., Inverno, C.M.C. and D'Orey, F.L.C. (2003b): Série Negra black quartzites – Tomar Cordoba Shear Zone, E Portugal: mineralogy and cathodoluminescence studies. *Cadernos do Laboratorio Xeolóxico de Laxe*, 28: 193-211.

de Oliveira, D.P.S., Robb, L.J., Inverno, C.M.C. and Charlesworth, E.G. (2007): Metallogenesis of the São Martinho and Mosteiros Gold Deposits, Tomar Cordoba Shear Zone, Portugal. *International Geology Review*, 49: 907-930.

Díez Fernández, R., Pereira, M.F. and Foster, D.A. (2014): Peralkaline and alkaline magmatism of the Ossa-Morena Zone (SW Iberia): Age, source and implications for the Paleozoic evolution of Gondwanan lithosphere. *Lithosphere*, 7: 73-90.

Dixon, T.H., Batiza, R., Fruta, K. and Martin, D. (1984): Petrochemistry, age and isotopic composition of alkali basalts from Ponape Island, Western Pacific. *Chemical Geology*, 43: 1-28.

Eguiluz, L., Ábalos, B. and Gil Ibarguchi, J.I. (1990): Eclogitas de la banda de Cizalla Badajoz-Cordoba (Suroeste de Espana). Datos petrográficos y significado geodinámico. *Geogaceta*, 7: 28-31.

Eguiluz, L., Gil Ibarguchi, J.I., Ábalos, B. and Apraiz, A. (2000): Superposed Hercynian and Cadomian orogenic cycles in the Ossa-Morena zone and related areas of the Iberian Massif. *Geological Society of America Bulletin*, 112: 1398-1413.

Flanagan, F.J. (1973): 1972 values for international geochemical reference samples. *Geochimica et Cosmochimica Acta*, 37: 1189-1200.

Folk, R.L. (1954): The distinction between Grain Size and Mineral Composition in Sedimentary-Rock Nomenclature. *The Journal of Geology,* 62(4): 344-359.

Gill, J. (1981): *Orogenic Andesites and Plate Tectonics*. New York, Springer-Verlag, 390 p.

Girty, G.H., Barber, R.W. and Knaack, C. (1993): REE, Th, Sc evidence for the depositional setting and source rock characteristics of the Quartz Hill chert, Sierra Nevada, California. *Geological Society of America (Special Paper)*, 284: 109-119.

Gómez-Pugnaire, M.T., Azor, A., Fernández-Soler, J.M. and Sánchez-Vizcaíno, V.L. (2003): The amphibolites from the Ossa–Morena/Central Iberian Variscan suture (southwestern Iberian Massif): Geochemistry and tectonic interpretation. *Lithos*, 68: 23-42.

Gonçalves, F. (1971): Subsídios para o Conhecimento Geológico do Nordeste Alentejano. *Memória Nº18*, Serviços Geológicos Portugal, 62 p.

Gonçalves, F., Assunção, C.T. and Coelho, A.V.P. (1972a): *Notícia explicativa da folha 33-C (Campo Maior)*. Serviços Geológicos Portugal, 41 p.

Gonçalves, F. and Carvalhosa, A. (1994): O Proterozóico da Zona de Ossa Morena no Alentejo. Síntese e actualização de conhecimentos. *Memórias Academia Ciências Lisboa*, XXXIV: 3-35.

Gonçalves, F. and Fernandes, A.P. (1973): *Notícia explicativa da folha 32-B (Portalegre)*. Serviços Geológicos Portugal, 45 p.

Gonçalves, F., Peleja, A.F. and Jardim, J.J. (1972b): *Carta Geológica de Portugal, nº 32-B (Portalegre), escala 1:50000*. Serviços Geológicos Portugal, Lisboa.

Gonçalves, F., Peleja, A.F., Pereira, M.A. and Bacharel, L. (1971): *Carta Geológica de Portugal, nº 33-C (Campo Maior), escala 1:50000.* Serviços Geológicos Portugal, Lisboa.

Gonçalves, F., Perdigão, J.C., Coelho, A.V.P. and Munhá, J.M. (1978): *Notícia explicativa da folha 33-A (Assumar)*. Serviços Geológicos Portugal, 37 p.

Herron, M.M. (1988): Geochemical classification of terrigenous sands and shales from core or log data. *Journal Sedimentary Petrology*, 58: 820-829.

Jödicke, H., Nover, G., Kruhl, J.H. and Markfort, R. (2007): Electrical properties of a graphite-rich quartzite from a former lower continental crust exposed in the Serre San Bruno, Calabria (southern Italy). *Physics of the Earth and Planetary Interiors,* 165: 56-67.

Krabbendam, M., Urai, J.L. and Vliet, L.J. van (2003): Grain size stabilisation by dispersed graphite in a high-grade quartz mylonite: an example from Naxos (Greece). *Journal of Structural Geology*, 25: 855-866.

Linnemann, U., Pereira, F., Jeffries, T.E., Drost, K., and Gerdes, A. (2008): The Cadomian orogeny and the opening of the Rheic Ocean: The diachrony of geotectonic processes constrained by LA-ICP-MS U-Pb zircon dating (Ossa-Morena and Saxo-Thuringian zones, Iberian and Bohemian Massifs): *Tectonophysics*, 461: 21-43.

Liotard, J.M., Barsczus, H.G., Dupy, C. and Dostal, J. (1986): Geochemistry and origin of basaltic lavas from Marquesas Archipelago, French Polynesia. *Contributions to Mineralogy and Petrology*, 92: 260-268.

McLennan, S.M., Hemming, S., McDaniel, D.K. and Hanson, G.N. (1993): Geochemical approaches to sedimentation, provenance and tectonics. *Geological Society of America (Special Paper)*, 284: 21-40.

McLennan, S.M., Taylor, S.R., McCulloch, M.T. and Maynard, J.B. (1990): Geochemical and Nd-Sr isotopic compositions of deep-sea turbidites: Crustal evolution and plate tectonic associations. *Geochimica et Cosmochimica Acta*, 54: 2015-2050.

Muhs, D.R. (2004): Mineralogical maturity in dunefields of North America, Africa and Australia. *Geomorphology*, 59: 247-269.

Nesbitt, H.W. and Young, G.M. (1982): Early Proterozoic climate and plate motion inferred from major element chemistry of lutites. *Nature*, 299: 715-717.

Oliveira, J.T., Oliveira, V. and Piçarra, J.M. (1991): Traços gerais da evolução tecto-estratigráfica da Zona de Ossa Morena. *Counicações dos Serviços Geológicos de.Portugal*, 77: 3-26.

Ordóñez Casado, B. (1998): Geochronological Studies of the Pre-Mesozoic Basement of the Iberian Massif: The Ossa Morena Zone and the Allochthonous Complexes within the Central Iberian Zone. Ph.D. Thesis, Zürich, Swiss Federal Institute of Technology, 235 p.

Pereira, M.F. (1995): Estudo tectónico da megaestrutura de Crato-Arronches-Campo Maior: A faixa Blastomlonítica e limite setentrional da Zona de Ossa Morena com o autóctone Centro Ibérico (Nordeste Alentejano). MSc Thesis, Faculty of Science, Univ. Lisbon, 108 p.

Pereira, M.F. (1999): Caracterização da estrutura dos domínios setentrionais da Zona de Ossa Morena e seu limite com a Zona Centro Ibérica, no nordeste Alentejano. Ph.D. Thesis, Évora Univ., Portugal, 114 p.

Pereira, M.F., Apraiz, A., Chichorro, M., Silva, J.B. and Armstrong, R.A. (2010): Exhumation of high-pressure rocks in northern Gondwana during the early Carboniferous (Coimbra-Cordoba shear zone, SW Iberian Massif): Tectonothermal analysis and U-Th-Pb SHRIMP in-situ zircon geochronology. *Gondwana Research*, 17: 440-460.

Pereira, M.F., Apraiz, A., Silva, J.B. and Chichorro, M. (2008): Tectonothermal analysis of high temperature mylonitization in the Coimbra-Cordoba shear zone (SW Iberian Massif, Ouguela tectonic unit, Portugal): Evidence of intra-continental transcurrent transport during the amalgamation of Pangea. *Tectonophysics*, 461: 378-394.

Pereira, M.F., Chichorro, M., Linnemann, U., Eguiluz, L. and Silva, J.B. (2006): Inherited arc signature in Ediacaran and Early Cambrian basins of the Ossa-Morena Zone (Iberian Massif, Portugal): Paleogeographic link with European and North African Cadomian correlatives. *Precambrian Research*, 144: 297-315.

Pereira, M.F. and Silva, J.B. (2000): Sinistral transcurrent transpression at the Ossa-Morena Zone/Central Iberian Zone boundary: the Portalegre-Esperança Shear Zone (Portugal). *Geogaceta*, 29: 131-134.

Puelles, P., Ábalos, B. and Fernández-Armas, S. (2013): Constraints on strain rate and fabric partitioning in ductilely deformed black quartzites (Badajoz-Córdoba Shear Zone, Iberian Massif). *Geophysical Research Abstracts* 15: EGU2013-1529.

Puelles, P., Ábalos, B. and Fernández-Armas, S. (2014): Graphite and quartz petrofabrics: examples from the Ediacaran black quartzites of the Ossa-Morena Zone (SW Iberia). *Tectonophysics*, 615-616: 53-68.

Quesada, C. (1991): Geological constraints on the Paleozoic tectonic evolution of tectonostratigraphic terranes in the Iberian Massif. *Tectonophysics*, 185: 225-245.

Rollinson, H.R. (1992): *Using geochemical data: Evaluation, Presentation, Interpretation*. Longman, 352 p.

Roser, B.P. and Korsch, R.J. (1988): Provenance signatures of sandstone-mudstone suites determined using discriminant function analysis of major-element data. *Chemical Geology*, 67: 119-139.

Schäfer, H.J., Gebauer, D., Nagler, T.F. and Eguiluz, L. (1993): Conventional and ion-microprobe U-Pb dating of detrital zircons of the Tentudía Group (Série Negra, SW Spain): implications for zircon systematics, stratigraphy, tectonics and the Precambrian/Cambrian boundary. *Contributions to Mineralogy and Petrology*, 113: 289-299.

Simancas, J.F., Tahiri, A., Azor, A., Lodeiro, F.G., Poyatos, D.J.M. and Hadi, H.E. (2005): The tectonic frame of the Variscan–Alleghanian orogen in southern Europe and northern Africa. *Tectonophysics*, 398: 181-198.

Solá, A.R., Pereira, M.F., Williams, I.S., Ribeiro, M.L., Neiva, A.M.R., Montero, P., Bea, F., and Zinger, T. (2008): New insights from U-Pb zircon dating of Early Ordovician magmatism on the northern Gondwana margin: The Urra Formation (SW Iberian Massif, Portugal): *Tectonophysics*, 461: 114-129.

Sugahara, H., Sugitania, K., Mimura, K., Yamashita, F. and Yamamoto, K. (2010): A systematic rare-earth elements and yttrium study of Archean cherts at the Mount Goldsworthy greenstone belt in the Pilbara Craton: Implications for the origin of microfossil-bearing black cherts. *Precambrian Research*, 177: 73-87.

Taylor, S.R. and McLennan, S.M. (1985): *The continental crust: Its composition and evolution*. Oxford, Blackwell Scientific Publications, 312 p.

Manuscrito recibido el 22-02-2016
Recibida la revisión el 18-07-2016
Aceptado el manuscrito revisado el 30-07-2016